THE GEOMORPHIC EVOLUTION OF LAVA PLAINS AT THE SPIRIT AND INSIGHT LANDING SITES: COMPARISON OF CRATER RETENTION AGES AND EROSION RATES USING HiRISE. S. A. Wilson[1*], N. Warner[2], J. Mueller[2], J. A. Grant[1], M. Golombek[3], C. Weitz[4] and M. Banks[5] [1]NASM CEPS, Smithsonian Institution, 6th at Independence SW, Washington, DC, 20560, *wilsons@si.edu, [2]SUNY Geneseo, Department of Geological Sciences, 1 College Circle, Geneseo, NY 14454, [3]Jet Propulsion Laboratory, California Institute of Technology, Pasadena, CA, California Institute of Technology, Pasadena, CA, [4]Planetary Science Institute, 1700 East Fort Lowell, Tucson, AZ, 85719. [5]NASA Goddard Space Flight Center, Greenbelt, MD.

Introduction: In 2018, the *InSight* mission landed in a degraded, ~400-700 Myr old, ~27 m-diameter (D), 0.3 m deep impact crater known as "*Homestead hollow*" (*HH*) [1-3] in Elysium Planitia [3-5]. Much of Elysium is characterized by smooth, basaltic lava plains estimated to be Hesperian (based on the size frequency distribution (SFD) of craters with D > 5 km) to Early Amazonian in age (based on the SFD of craters with diameters between 200 m and 1 km [e.g., 6]). Nearly 15 years prior, the Mars Exploration Rover *Spirit* also landed on basaltic lava plains in Gusev crater that are Late Hesperian to Amazonian in age [e.g., 7-9]. Along its traverse, *Spirit* investigated several sediment-filled hollows that are comparable in size and appearance to *HH* [10-12] yet many appear to retain better-preserved rims (e.g., less degraded) (**Fig. 1**).

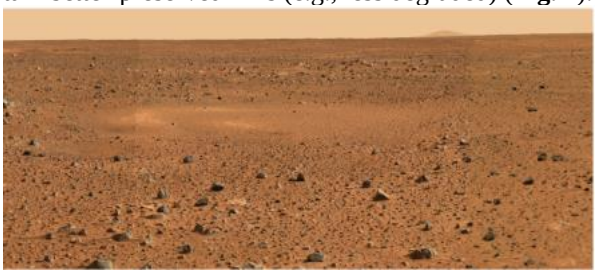

Figure 1. Example of a D ~10 m sediment-filled hollow in Gusev. Pancam mosaic image Sol029A_P2381_L247atc (modified from [12]).

Background: Previous work at *InSight* [3, 6] using images from the High-Resolution Imaging Science Experiment (HiRISE) [13] (~0.25 m/pixel resolution) established a crater classification system and degradational continuum (Class 1 are pristine craters, down to Class 8 which are degraded hollow-like craters). Crater morphology was combined with a morphometric analysis using a HiRISE digital elevation model (DEM) (1 meter per elevation posting) to estimate the erosion rates for relatively fresh, 10 to 100-m-scale craters across the entire final *InSight* landing ellipse.

Study Motivation: Despite the broad similarities between the *Spirit* and *InSight* landing sites, the craters at the *Spirit* landing site have not yet received the same analyses using HiRISE data. Using comparable datasets and techniques as [3, 6], we aim to understand if the populations of degraded craters and quasi-circular depressions on the floor of Gusev crater follow the same degradation continuum as observed at the *InSight* landing site. The comparison between Gusev and Elysium will further our understanding of the degradation history of craters on Hesperian- to Early Amazonian-aged volcanic surfaces and provide constraints on the timing and extent of burial and exhumation events.

Methods: Craters were mapped using HiRISE in a 21 km^2 area (same size area as was examined in Elysium [6]) around the *Spirit* landing site and classified based on their state of degradation (Class 1-8) after [3, 6] (**Fig. 2**).

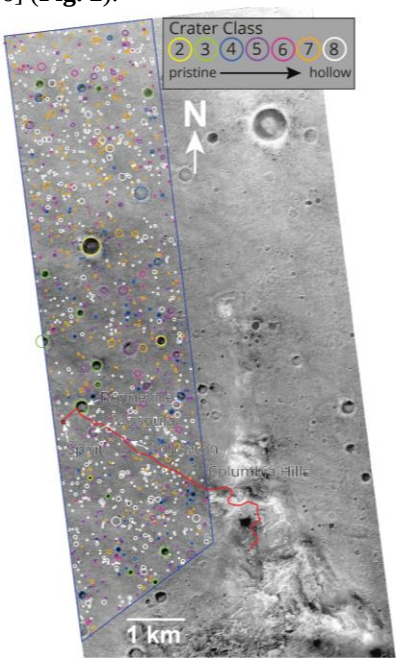

Figure 2. Craters counted and classified by degradation state (Class 1-8) in the 21 km^2 area (blue line) around the *Spirit* landing site (red dot) in Gusev. Red line marks the rover traverse across the lava plains to the Columbia Hills. Major craters labeled. HiRISE ESP_049643_1655.

Crater statistics were compiled using CraterTools [15], in ArcGIS. Relative ages of the surfaces were interpreted from cumulative plots created in Craterstats software, using the Mars chronology function of [16], production function of [17], and the equilibrium function of [18]. The morphometric analysis using a corresponding HiRISE DEM (DTEEC_049788_1655_049643_1655_U01) was used to measure crater morphometry, a means of capturing the continuum of crater degradation and erosion through time (parameters include diameter, maximum depth, maximum rim height, maximum slope, mean curvature, and mean roughness).

The maximum crater depth was calculated by fitting a 3D plane across the rim. Each point is assigned an elevation value from the HiRISE DEM, and then the DEM is subtracted from the overlying 3D surface. Crater rim height raster (1 m per pixel) with the 0.2D annular region was applied for each crater (this generally defines the majority of the rim structure for all craters). Rim height is calculated by fitting a plane across the continuous ejecta blanket (1D from crater rim). This 3D plane defines the pre-impact surface and is subtracted from the overlying DEM.

Preliminary Results: At the *Spirit* landing site (**Fig. 2**), we mapped 1,419 craters with diameters ≥ 20 m (D ranges from 20 m to 282 m). Compared to the 2,260 total craters (D≥20 m) mapped at Elysium, the Gusev plains appear relatively younger. The SFD of the Class 8 hollows in Gusev is consistent with an impact origin (**Fig. 3**). Craters at all diameters less than 100 m generally follows the -2 slope that is similar to the equilibrium function of [18], but smaller diameter craters roll off the curve due to erosional losses. The cumulative frequencies of Class 8, *HH*-size (~27 m in diameter) features in Gusev provide Mid to Late Amazonian model age of 300 ± 10 Myr (D ≥ 25-m bin) relative to 680 ± 20 Myr at the *InSight* landing site.

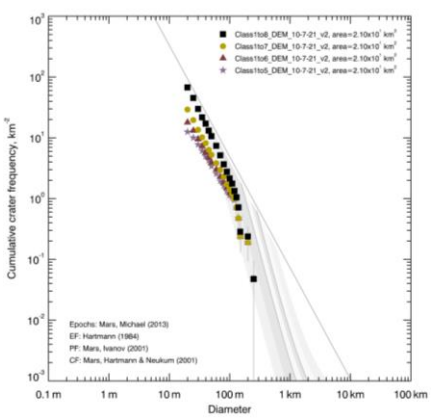

Figure. 3. Cumulative SFD showing the distribution for Class 1-5 (purple), Class 1-6 (red), Class 1-7 (yellow), and Class 1-8 (black) craters around the *Spirit* landing site in Gusev (see Fig. 2).

Crater degradation rates are determined using the interpreted time intervals between classes of a specific diameter bin and the changes to crater depth at that same bin [6]. In Gusev, the average maximum depth of a *HH*-sized crater (the 25 m- diameter bin) decreases (from 1.08 m to 0.44m) as degradation class increases from Class 5-8, yielding degradation rates of 1.1×10^{-2} m My^{-1} (Class 5-6), 6.2×10^{-3} m My^{-1} (Class 6-7), and 9.2×10^{-4} m My^{-1} (Class 7-8) – slightly higher than at the *InSight* landing site [3, 6] (**Fig. 4**). Reduction in rim height, which is the best proxy for landscape erosion, for each diameter bin were determined between the classes and integrated with the estimated retention ages at the same bin to provide a rim erosion rate [3, 6]. In Gusev, the average maximum rim height of a *HH*-sized crater (the 25 m- diameter bin) decreases (from 1.01 m to 0.47m) as degradation increases from Class 5-8. Rim erosion rates are 9.9×10^{-3} m My^{-1} (Class 5-6), 3.6×10^{-3} m My^{-1} (Class 6-7), 1.1×10^{-3} m My^{-1} (Class 7-8) – slightly higher than at the *InSight* landing site [3, 6] (**Fig. 4**).

Degradation rate (m My^{-1})		
	Gusev	InSight
Class 5 to 6	1.1×10^{-2}	4.6×10^{-3}
Class 6 to 7	6.2×10^{-3}	1.2×10^{-3}
Class 7 to 8	9.2×10^{-4}	3.6×10^{-4}
Rim erosion rate (m My^{-1})		
	Gusev	InSight
Class 5 to 6	9.9×10^{-3}	2.5×10^{-3}
Class 6 to 7	3.6×10^{-3}	1.6×10^{-3}
Class 7 to 8	1.1×10^{-3}	4.1×10^{-4}

Figure. 4. Relative degradation and rim erosion rates for a *HH*-size crater (25 m-D bin) at Gusev and *InSight*.

Discussion: The comparison between Gusev and Elysium will help further our understanding of the degradation history of craters on Hesperian to Early Amazonian volcanic surfaces, and may provide clues about the timing and extent of burial and exhumation events. The estimated maximum age for hollows (D≥25-m bin) at the *Spirit* landing site are slightly younger relative to the estimated maximum age of hollows at the *InSight* landing site, and the crater degradation and rim erosion rates are relatively higher. This may be due to the intensity of aeolian processes and (or) differences in the composition of surface material. Younger surface in Gusev may account for the observation that craters appear to have better preserved rims, but the competing factor is the higher rates of degradation and erosion: perhaps the higher rates may not completely compensate for the younger surface, or the age of the surface is more important than the degradation rates.

References: [1] Golombek, M.P., et al. (2020) Nat. Comm., 11 [2] Grant, J.A., et al. (2020) JGR, 125 [3] Warner, N.H., et al. (2020) JGR, 125. [4] Banerdt, W. B., et al. (2020). Nat. Geosci., 13 [5] Golombek, M., et al. (2020) ESS, 7 [6] Sweeney, J., et. al. (2018) JGR, https://doi.org/10.1029/2018JE005618 [7] Cabrol, N. A., et al., (1998), JGR, doi:10.1029/2002JE002026 [8] Kuzmin, R. O., et al. (2000), Geologic Inv. Series, 8, pp., USGS [9] Milam, K. A., et al., (2003), JGR, doi:10.1029/2002JE002023 [10] Grant et al. (2006), JGR, doi:10.1029/2005JE002465 [11] Golombek, M. P., et al. (2006), JGR, doi:10.1029/ 2005JE002503 [12] Weitz et al (2021), JGR, DOI:10.1029/2020JE006435 [13] McEwen et al. (2007), JGR, doi:10.1029/2005JE002605. [14] Malin et al. (2007), JGR, doi:10.1029/2006JE002808. [15] Kneissl, T., et al. (2011), PSS [16] Hartmann, W. K., G. Neukum (2001), SSR, doi:10.1023/A:10119452220 [17] Ivanov, B.A. (2001), SSR doi:10.1023/A:1011941121102 [18] Hartmann, W.K. (1984), Icarus, 60, 56–74.